

Chapter 12

From MEMS to NEMS



Teodor Gotszalk

12.1 Introduction

Nanotechnology, as the scientific and technological discipline dealing with the design, fabrication and application of systems whose dimensions or tolerances are in the domain of nanometers, is becoming increasingly important in many industrial and scientific areas. Nanotechnologies and nanoscience are triggered by diverse fields and applications but on the other hand, they trigger by themselves future industrial and practical solutions. One of the most important challenges observed nowadays in nanotechnology is driving the manufacturing processes to sub-nm accuracy level for critical features and positioning tasks.

The progress in nanotechnology is directly connected with the progress in the Micro-Electro-Mechanical Systems (MEMS) technology, which in many countries is also called as the Microsystems technology. In general it can be described as the technology of miniaturized electro-mechanical devices and structures that are fabricated using technologies used for fabrication of semiconductor integrated circuits (ICs). To the MEMS belong simple devices like supported beams (cantilevers), double-clamped microbridges and membranes as well as complicated structures with moving mechanical components, whose deflection is precisely detected and controlled. In the most mature form the electromechanical components are integrated with microcontrollers, which perform not only simple operations but enable implementation of artificial intelligence (AI) algorithms.

The critical physical dimensions of the MEMS can vary from several microns to several millimeters. The attractiveness of the MEMS technology is intuitive—the small dimensions of the MEMS device make the MEMS device sensitive to phenomena occurring at micro- and nanoscale. In other words the smaller structure one wishes to observe the smaller tool must be used. Moreover, as the MEMS are fabricated in the so called batch processes, their cost can be reduced and the scale of integration increased, leading to the increase of the observation throughput. It should be noted however, that the MEMS are distinct from the idea of the molecular electronics and molecular nanotechnology. In principle, the MEMS are fabricated in the so called

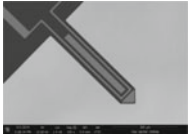
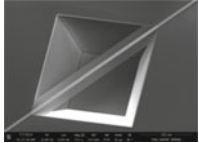
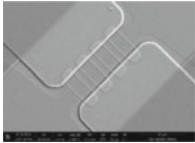
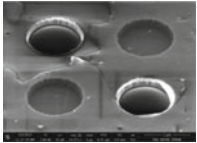
top-down processes, in which a device is assembled by various processes shaping the final mechanical and electrical device form. In contrast, bottom-up processes, are based on the chemical properties of individual species, which cause single-molecule components to self-organize and/or self-assemble into some useful conformation. It should be noted however, that the MEMS make it possible to manipulate with single molecules and from that point of view the MEMS are of huge importance for the bottom-up technology.

In the natural way the MEMS technology merges at the nanoscale into Nano-Electro-Mechanical-Systems (NEMS). The experimental possibilities are in this case even bigger as the tool dimension size is reduced [15]. Challenge of the today's MEMS/NEMS technology is that it does not only involve application of modern microfabrication techniques but also require thorough analysis of the system operation. The analysis based on classical physics cannot often be used to describe and interpret the phenomena defining the functionality of a MEMS/NEMS device. At these scales of dimensions the large surface area to volume ratio of the MEMS devices, surface effects such as electrostatics, wetting, molecular adhesion, which includes chemical interactions, dominate volume effects such as inertia or thermal mass. Due to very small device dimensions and tiny distances between the device components, which are being moved, quantum phenomena must be taken into account in order to describe the recorded phenomena. This in turn makes the interpretation of the observed MEMS/NEMS behavior distinct from the interpretation the engineers are today accustomed to. In Table 12.1 a group of MEMS/NEMS devices is presented illustrating the described tendency. The list begins with a MEMS cantilever whose actuation is driven electromagnetically [26]. The spring beam is formed out of crystalline silicon, a metal thin film loop is used to actuate the structure deflection. The simplest way to fabricate the structures whose thickness is of hundreds of nanometers is to form them out of a thin film. In this way the mass of the structure can be reduced as in case of the silicon nitride microbridges [23]. Silicon nanowires are one the next NEMS device examples [38]. When released out of the substrate they can act as nanoresonators. The most important feature of the proposed architecture is that each of the wires integrated in an array can be addressed separately, which increases the operation throughput, as the response of every wire can be sensed separately.

Besides classical materials utilized and applied in micro- and nanoelectronics, there are also attempts to apply the 2 dimensional (2D) crystals as the materials for the MEMS and NEMS devices. In such a setup, the atomically thick membranes form the NEMS mechanical part. Excellent material properties of 2D structures make such systems very attractive [4, 5, 8].

As the MEMS/NEMS devices have been developed and applied, more and more frequently progress in their metrology has been also observed. Metrology is defined as the science of measurement including all practical and theoretical aspects. It is essential for scientific research and development (R&D) as well as for technological innovation. High quality metrology is critical to the major advances in all scientific fields. Moreover, metrology supports modern industrial competitiveness and development of new and improved products and processes.

Table 12.1 MEMS and NEMS devices-dimensions and mass

MEMS electromagnetically actuated cantilever		MEMS Silicon nitride microbeam	NEMS Silicon nanowires	Graphene based NEMS membranes (GNEMS)
				
Length (μm)	600	600	5	10
Thickness	10 μm	100 nm	50 nm	Non-defined
Mass	50 ng	50 pg	50 fg	Non-defined

Lord Kelvin quoted in 19th century: “If you cannot measure it, you cannot improve it”, which means that without reliable measurements, we do not understand properly and cannot control, manufacturing process in the reliable manner. Thus, advances in metrology and their effective use have a profound impact on our understanding of and ability to shape the world around us.

Moreover, it must be said that: not only is progress in nanotechnology, nanoscience and microsystem technology enabled due to the headway made in nanometrology but it also stimulates the development of measurement methods and techniques. This bidirectional relation makes the metrology research unique and of very high interest for almost all scientific fields.

Limitation of the today metrology is that the procedures, applied by National Metrological Institutes (NMIs) and introduced in the everyday practice, are mostly based on classical theorems (including classical elasticity theory, classical electrodynamics, thermodynamics etc.). It is clear, that because of the progress in miniaturization the role of the so called Quantum metrology will be increasing continuously. The first symptoms of this tendency, involving the introduction of the Josephson voltage, Hall quantum resistance reference standards, have been already indicated but it is evident to us that the more basic orientated research on this field will be necessary so that to make the mentioned theories accessible for wider group of scientist and technicians.

12.2 NEMS Sensitivity and Resolution

The vibrating MEMS/NEMS can be described basing on the simple harmonic oscillator (SHO) equation:

$$m \frac{\partial^2 x(t)}{\partial t^2} + \gamma \frac{\partial x(t)}{\partial t} + kx(t) = 0 \quad (12.1)$$

where m is the MEMS/NEMS mass, γ is the damping ratio and k is the MEMS/NEMS stiffness, x is the structure deflection. The above equation can be rewritten as:

$$\frac{\partial^2 x(t)}{\partial t^2} + \frac{\omega_0}{Q} \frac{\partial x(t)}{\partial t} + \omega_0^2 x(t) = 0. \quad (12.2)$$

where $Q = \frac{\sqrt{km}}{\gamma}$ is the quality factor and ω_0 is the angular frequency of the free structure vibration: $\omega_0 = \sqrt{\frac{k}{m}}$.

In many investigations MEMS/NEMS are used as resonators, which means that the deflection is excited by the external force, in this case:

$$\frac{\partial^2 x(t)}{\partial t^2} + \frac{\omega_0}{Q} \frac{\partial x(t)}{\partial t} + \omega_0^2 x(t) = \frac{f(t)}{m}. \quad (12.3)$$

where $f(t)$ is the force applied to a MEMS/NEMS to excite its vibration. The displacement $x(t)$ can be derived in frequency domain by Fourier transforming of Eq. (12.3):

$$X(j\omega) = \frac{F(j\omega)}{m} \frac{1}{(\omega_0^2 - \omega^2) + j\frac{\omega\omega_0}{Q}}, \quad (12.4)$$

where $F(j\omega)$ and $X(j\omega)$ are Fourier transforms of the force and MEMS/NEMS displacement respectively.

As investigations are usually performed using a network/spectrum analyzer in frequency space, the presented analysis in which MEMS/NEMS response is analyzed in frequency domain is very useful. Moreover, the recorded response signal can be split into real and imaginary or amplitude and phase components, which opens a field for a variety of detection techniques.

When Lorentz fitting is applied, the radial resonance frequency (ω_r), can be accurately determined. The full width at half maximum ($\Delta\omega$) is related to the damping coefficient γ . In all the mentioned above experiments the force F is related to the actuation technology, responsible for excitation of MEMS/NEMS movement. It's worth noticing, that the resonance frequency can be calculated as:

$$\omega_r = \omega_0 \sqrt{1 - \frac{1}{2Q^2}}. \quad (12.5)$$

However, it should be also noticed that for high quality factors the angular frequency of free vibration is almost equal to the structure resonance frequency. Quality factor, which is the measure of the energy dissipation, influences the dynamics of the signal phase as well:

$$\varphi = \tan^{-1} \left(\frac{\omega\omega_0}{Q(\omega_0^2 - \omega^2)} \right). \quad (12.6)$$

12.2.1 Resolution and Sensitivity of MEMS/NEMS Devices

Two parameters of a MEMS/NEMS device are important to describe its properties: the sensitivity and the resolution. The sensitivity of a measuring system is the quotient of the change in an indication of a measuring system and the corresponding change in a value of a quantity being measured [29].

If a MEMS/NEMS device is applied as a mass change sensor the most efficient way to observe its sensitivity is to observe device resonance frequency, which is described by equation: $\omega_0 = \sqrt{\frac{k}{m}}$. Moreover, from technical point of view detection of small frequency changes can be performed with the highest precision, stability and accuracy using a modern phase locked loop (PLL) circuitry. If we differentiate the above formula the following formula describing mass change sensitivity can be obtained:

$$\frac{\partial\omega_0}{\partial m} = -\frac{1}{2} \frac{\omega_0}{m}, \quad (12.7)$$

which clearly shows that a higher mass change sensitivity is obtained when a MEMS/NEMS device of small mass exhibits high resonance frequency.

For the doubly clamped bridge, taking into account that its resonance radial frequency ω_{0b} and the effective mass m_b can be calculated basing on the following formulas: $\omega_{0b} = 2\pi \cdot 1.05 \frac{l}{l^2} \sqrt{\frac{E}{\rho}}$ and $m_b = 2 \cdot 0.73wl\rho$, the mass change sensitivity can be written as:

$$\frac{\partial\omega_{0b}}{\partial m_b} = 2.25 \frac{1}{wl^3} \sqrt{\frac{E}{\rho^3}}. \quad (12.8)$$

with E, Young's modulus, ρ , mass density, w , bridge width and l , bridge length.

According to this formula the mass change detection sensitivity increases when factors $\sqrt{\frac{E}{\rho^3}}$ and $\frac{1}{wl^3}$ are maximized. In consequence materials forming a MEMS/NEMS device of high elasticity and low mass density are of big interest. In this case that the silicon carbide structures should exhibit 1.5 better sensitivity than the silicon devices. Moreover, devices of small length and width are preferable.

Similar analysis of the mass change detection sensitivity can be done for the supported beam-cantilevers, which leads to analogous conclusions. In general structures of low stiffness and high resonance frequencies are the most sensitive.

The performed above analysis indicates that the 2D NEMS structures are of big importance for the modern sensor technology. A NEMS device formed out of 2D

material exhibits extremely high Young modulus, which results from the atomic structure of the vibrating components. In this case, if the structure does not contain any defects the 2D NEMS elasticity is the results of atomic bonds between atoms forming the movable NEMS part [2, 21].

The density of such a mechanical part is very low, as in the ideal case the movable components are built only out of atoms. Although, at this place difficulties in the interpretation of the observed phenomena, especially taking into account classical theories of the mechanical and electrical engineering, must be noticed.

In general, if an elastic structure is being deformed by an external force, it experiences internal resistance to the being induced deformation and restores it to its original state if the external force is no longer applied. There are various material parameters: the so-called elastic moduli, such as Young's modulus, the shear modulus, and the bulk modulus, which describe the inherent elastic behavior of a structure as a resistance to deformation under an applied load. The mentioned moduli apply to different kinds of deformation, e.g. Young's modulus applies to extension/compression of the body, whereas the shear modulus applies to its shear.

The elasticity of a structure is exactly described by a stress-strain characteristic, which is the relation between the so-called stress (which is the ratio of average restorative internal force over unit area) and strain (which is the relative structure deformation). In general, the characteristics is nonlinear, but by use of a Taylor series it can be approximated as linear for sufficiently small deformations (which means, that the higher-order terms can be neglected).

The linearized stress-strain relationship is described by the Hooke's law, which is usually applied to the elastic limit for most metals or crystalline materials. It must be noted additionally, that because in general stresses and strains can have various independent components the proportionality factor can no longer be just a single number but rather a tensor containing real numbers (e.g. defined for various crystallographic directions). Moreover, Young's modulus is the technical parameter resulting from interaction in continuum structure: it is therefore an average of various atomic and molecular interaction which internally occur in the being deformed body.

This classical approach can and is very often applied in the MEMS analysis, which are big enough to be described with global parameters like e.g. Young's modulus. However if the analysis of NEMS is considered, the fundamental questions arise if this approach can be applied for structures, whose thickness corresponds to the atoms or molecules which can be sometimes even counted. The most exact approach is in this case to calculate elastic properties *ab initio*, in other words *from the first principles*, manner. An *ab initio* calculation starts in this case with the properties of constituent atoms forming e.g. graphene flake and the laws of quantum mechanics. In general the characteristics of isolated individual molecules can be derived and consequently followed by computations of the interactions of larger and larger groups of molecules and as a result the properties of the entire NEMS structure can be calculated. When real structures are taken into consideration, e.g. polycrystals, containing defects, supported or suspended on bulk holders, the *ab initio* calculations are extremely difficult, time and labor consuming. The obtained results are quite often not the intuitive ones and from the NEMS design and interpretation point of view not helpful.

Moreover, in MEMS and NEMS analysis it is essential that the terms stress and strain must be defined without ambiguity. If NEMS are considered, the structure deflection is usually of fractions of nanometers and is observed quite often in the frequency bandwidth of up to 100 MHz. This creates a lot of technical problems in the deflection detection and if the metrology is considered the procedures are even more difficult.

The second parameter describing metrology using a MEMS/NEMS device is its resolution described as the smallest change in a quantity being measured which causes a perceptible change in the corresponding indication [29].

The analysis of the MEMS force measurement resolution illustrates the general rules governing the way how to improve the system parameters. In the MEMS/NEMS technology the static force is observed by the detection of the spring beam static deflection. In general stochastic vibration of the MEMS/NEMS molecules and the vibration of the molecules around a system form background of the force interaction observations. In analogy with electrical engineering, when one assumes that the force is the analogy to the electrical voltage and MEMS/NEMS speed corresponds with the electrical current the minimum detectable force F_{\min} can be calculated like Johnson-Nyquist noise:

$$F_{\min} = \sqrt{4k_B T \gamma B}, \quad (12.9)$$

where k_B is the Boltzman constant, T is the MEMS/NEMS temperature, B is the measurement bandwidth. If we notice that $\gamma = \frac{k}{\omega_0 Q}$ and assume that Q is high enough, which makes that ω_r and ω_0 are equal, the formula for the minimum detectable force is:

$$F_{\min} = \sqrt{\frac{4k_B k T B}{Q \omega_0}} = \sqrt{\frac{2k_B k T B}{\pi Q f_0}}, \quad (12.10)$$

where f_0 is the free vibration frequency. It can be clearly seen, that the cantilevers of small stiffness and high free vibration frequency exhibit higher resolution of force detection. For the MEMS cantilever presented in Table 12.1 with the stiffness of 15 N/m, resonance frequency of 50 kHz, the smallest detectable force is 42 fN/Hz^{0.5} in the bandwidth of 1 Hz but for the silicon NEMS cantilever with 20 μm length, 0.3 μm thickness and 10 μm width, corresponding with stiffness of 1.7 N/m and resonance frequency of 320 kHz, the minimum detectable force can be reduced to 7 fN/Hz^{0.5} (both parameters were calculated for quality factors of 300 and ambient temperatures). When the measurements are done in liquid nitrogen (LN) and vacuum, which usually leads to quality factor increase to 10,000, the minimum detectable force is reduced to 60 aN/Hz^{0.5}.

Another very important issue, illustrating the capabilities of the NEMS devices is the small operating power P_{\min} needed for their activation. For a resonant MEMS/NEMS power P_{\min} can be calculated by noticing that the device is a lossy energy storage. Energy injected into the device is dissipated in a time:

$$\tau \approx \frac{Q}{\omega_0} \quad (12.11)$$

which is often named as the ring-down time of the resonator. The minimum operation energy for the system is the energy, which will drive the NEMS at amplitude corresponding with the thermal fluctuation. Given the energy $k_B T$ of the mode thermal fluctuation the minimum power P_{\min} can be estimated in this case as:

$$P_{\min} \approx \frac{k_B T}{\tau} = \frac{k_B T \omega_0}{Q}. \quad (12.12)$$

For a NEMS device which can be fabricated using today's technologies the minimum power P_{\min} is on the order of tens of aW (10^{-17} W). One can estimate that even for the systems operating with arrays containing thousands of NEMS resonators, the minimum power needed for the operation is far smaller than for the electronic devices, in which power of several microwatts is usually dissipated.

12.2.2 NEMS Fabrication Technology

The vast majority of technologies applied in fabrication of NEMS devices is based on microfabrication procedures applied in the manufacturing of microelectronic integrated circuits (ICs). A lot of various techniques including etching, lithography, thin film deposition, resist processing are available in the research laboratories. However complexity and difficulties, connected mostly with the fabrication of structures whose dimensions are in the range of tens of nanometers, must be mentioned. To the most time consuming, cost and equipment involving processes belong electron beam (E-beam) lithography, deep silicon etching and integration with application specific integrated circuits (ASICs). The described above methodology can be applied in single wafer or batch processing and the latter one is the cost-effective method of dealing with volume manufacturing. One of the ways enabling manufacturing of the prototype NEMS is to fabricate the device out of thin film deposited on solid substrate e.g. silicon wafer. In this way application of costly silicon on insulator (SOI) or silicon carbide (SiC) substrates as well as expensive deep silicon etching processes will be avoided [18].

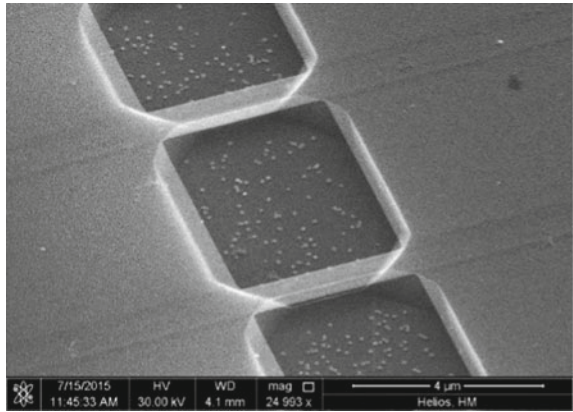
In the proposed technology silicon nitride NEMS bridges were fabricated [25]. In order to enable detection and actuation of NEMS vibration metallization paths were integrated with moveable components. In general fabrication of silicon nitride films of thickness less than 200 nm is difficult due to high tensile stress occurring while thin film deposition. As the result the adhesion between silicon nitride and silicon is small, leading to the structure instability. However, by the process parameters optimization (changing of the substrate temperature, gas flow, gas ratio, pressure and time) it was possible to produce thick silicon nitride and deposit a layer resist for wet etching in KOH solution.

The entire fabrication process of the NEMS bridge consists of three steps. In the first fabrication step a stoichiometric silicon nitride Si_3N_4 layer (200 nm in thickness) is deposited in LPCVD method with $(\text{SiH}_2\text{Cl}_2/\text{NH}_3)$ gas ratio of 1:4. The stoichiometric LPCVD nitride shows a very large tensile stress (~ 1.7 GPa) and is compensated by a subsequent non-stoichiometric silicon nitride deposition. The non-stoichiometric silicon nitride Si_xN_y (200 nm in thickness) was deposited with $\text{SiH}_2\text{Cl}_2/\text{NH}_3$ gas ratio of 8:1. The conducted process results in the reduction of the stress in the deposited layer forming a NEMS bridge to ca. 0.2 GPa. In the second fabrication step chromium (as an adhesion layer) and platinum layers were sputtered. In a dry plasma etching process of the platinum and the silicon nitride the metallization paths and shapes of the NEMS bridge are defined. Finally the structures are released by wet etch silicon in KOH solution. A variety of NEMS bridges with thickness of up to 500 nm, width of 50 μm and length of 420 μm were fabricated in this scenario. All the structures were wire-bonded to the printed circuit boards (PCB) which made it possible to detect and actuate structure vibrations. The silicon nitride bridge, fabricated in the above described technology, of dimensions: length 280 μm , width 40 μm and for the Young modulus of 160 GPa, and silicon nitride density of 2700 kg/m^3 exhibits mass change density calculated according to Eq. (12.8) of 1.24 MHz/ag.

It must be noted however, that even if the NEMS fabrication process is simplified it is still challenging. According to the state of the art, NEMS solutions are based on electron beam (E-beam) lithography and following quite complicated etching steps associated with depositions and photolithography procedures. Such an approach is extremely expensive in terms of process complexity, characterization, instrumentation and very time-consuming. Moreover, in this way fast prototyping needed, when the possibilities of the NEMS tool should be assessed are very limited, as in the standard process only the wafer scale manufacturing is possible. One of the solutions to these problems is the application of focused ion beam (FIB) and scanning electron microscopy (SEM) based techniques. In the standard approach, the FIB and SEM technologies, forming the so called dual platform systems (integrating both ion and electron beam columns), have been widely used for microfabrication, nanofabrication and testing of the IC's. The focused gallium ions and electrons are directed onto the samples and applied to modify or image the investigated sample. In this way FIB and SEM tools can sputter and implant lines as narrow as 20 nm and deposit metals and insulators in lines as narrow as 20 nm in user-defined patterns.

The focused electron beam and scanning electron microscopes have been extensively used for the fabrication of the transmission electron microscopy (TEM) sample preparation. In this case the beam of gallium ions carry enough energy to make the sample so thin that it will be transparent for the electrons in a transmission electron microscope. What must be underlined is that the process can be controlled with precision and resolution of fractions of nanometers. That is the reason why both technologies have attracted much interest in the fabrication of NEMS devices. The most straightforward procedure is to use highly energetic gallium ions for modification (milling down) MEMS devices. In this way sensors for scanning near field optical microscopy (SNOM) were successfully fabricated by opening an aperture of tens of

Fig. 12.1 NEMS silicon nanobridge fabricated using FIB technology; silicon bridges were patterned with gallium ion beam and wet etched; bridge thickness ca. 30 nm; estimated device mass 10 fg



nanometers opening in the microtip [10]. The FIB milled SNOM nanoprobe is only an example of the application of the described technology in the nanotools experiments. There are other examples, in which MEMS as basic structures were applied and by the milling done at the defined positions nanotip cantilevers for advanced scanning probe microscopy (SPM) or tiny calibration references were fabricated.

Besides ion milling there is another nanofabrication technology which relies on gallium ion FIB implantation. In this case when on a silicon crystal sample a beam of gallium ions is directed the implanted areas form a structure which is resistant to subsequent etching in KOH solution (in other words the implanted areas are an etch stop structures in wet etching procedure). The etch stop technology has been known in microelectronics for almost 2 decades but it was applied in the FIB technology by Murano group for the first time [20]. In this way 3 dimensional (3D) structures can be created, whose dimensions are of tens of nanometers. In Fig. 12.1 a set of gallium implanted silicon nanobridges is presented. As it can be seen, the silicon crystal walls are clearly visible which is typical for the wet etching process. The nanobridge structures are of 30 nm thickness, which makes the structure almost transparent for the electrons used for SEM imaging. The estimated nanobridge mass is of 10 fg, which is almost three orders of magnitude smaller mass than the mass of silicon nitride nanobridges presented in Table 12.1.

The described technology makes it possible to fabricate a variety of NEMS and is very attractive for the single devices or prototype investigations. It was also utilized in the fabrication of the array NEMS [19].

The FIB/SEM technology enables also fabrication of 3D nanostructures in the so called focused electron beam induced deposition (FEBID) process. In this scheme the investigated structure is immersed in environment of metal organic (MeO) precursor. On the areas exposed to the electron beam, metal (Me) containing structures can be deposited. In contrast to FIB milling, which is the top-down procedure (a manufactured structure is fabricated out of the larger part) FEBID process is the bottom-up

procedure (which means that the particular components are being integrated to give rise to more complex systems).

The FEBID technology is a mask-less deposition technique suitable for NEMS rapid prototyping. The deposition process can be performed faster and in the more flexible way than in conventional microelectronics fabrication processes. As the dimensions of the fabricate devices correspond to the resolution of a scanning electron microscope the metal containing structures can be placed with resolution of tens of nanometers. There is a variety of metal containing precursors which are used in FEBID technology. The conductive wires are fabricated basing on platinum, gold, cobalt or silver [3, 11, 16, 30]. FEBID technology makes it not only possible to fabricate high frequency (HF) resonators but also devices or components for NEMS deflection detection. In this case solutions based on field emission (FE) and piezoresistivity can be basically distinguished (further details can be found in the chapter on NEMS deflection detection methodology).

An important concept of the metrology is the traceability, which means that the result of a measurement must be related to stated references through an unbroken chain of comparisons with stated uncertainties. In case of the above-described NEMS-deflections investigations, there is lack of reliable and easily accessible calibration routines which leads to discrepancies in the assessment of various experiments. In this way FEBID technology was applied to verify the NEMS mass change detection resolution, which can be estimated using Eq. (12.8). To perform such an experiment NEMS device must be loaded with the mass which is known and the resonance frequencies before and after mass loading must be measured. In Fig. 12.2 platinum/carbon FEBID lines deposited on a silicon nitride bridge (Table 12.1) are visible. As it can be estimated from atomic force microscopy (AFM) image the line height and line width is of 50 and 20 nm respectively (see Fig. 12.3). In this way the mass of ca. 7 pg can be calculated which leads to the resonance frequency shift of 1324 Hz. The experimentally verified mass change detection resolution is of 0.18 Hz/fg. The differences between theoretically calculated and verified parameters stem from many reasons and illustrate very well the problems of nanometrology performed with NEMS tools. It should be noted that, Young's modulus of the silicon nitride and thin film metallization films cannot be described precisely and are technology and process dependent. Moreover, shape of the bridge anchoring points, due to the crystal structure of the silicon substrates, make elasticity calculations very difficult or almost completely impossible. The density of platinum/carbon FEBID reference structures depends on the way how the FEBID process is performed. Despite all these difficulties, the proposed routine makes it possible to confirm the sensitivity of the mass change detectors based on silicon nitride bridges.

As it was mentioned previously besides the sensor sensitivity the second parameter describing a NEMS device is its resolution. In the simplest approach, the resolution of the resonance frequency corresponds with the resolution of the system using which the vibration amplitude or phase are observed. The higher resolution of the mass change detection can be achieved when a NEMS resonator vibrates with high quality factor Q . In this case the bandwidth of the resonance frequency Δf can be estimated using equation $\Delta f = f_0/Q$, and for typical silicon nitride bridges

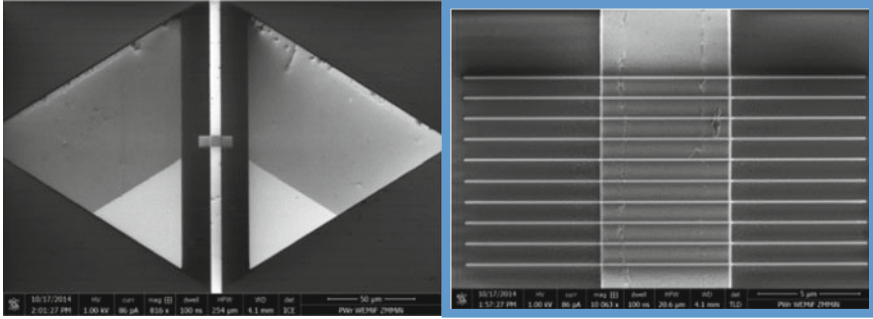
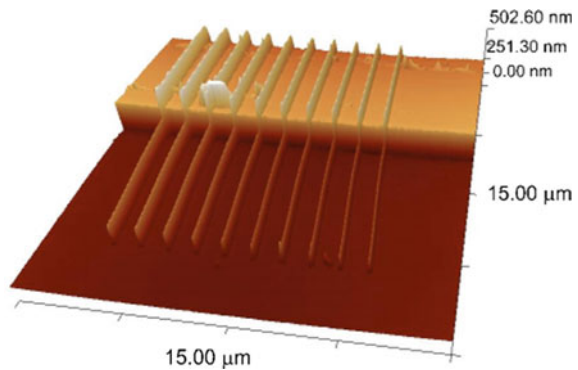


Fig. 12.2 NEMS silicon nitride bridge with FEBID deposited structure for mass-change detection-sensitivity calibration

Fig. 12.3 AFM image of the FEBID calibration structures used to calibrate the mass change sensitivity



presented in Table 12.1 it is of hundreds of hertz for measurements performed in ambient conditions. The higher quality factors can be achieved when the dissipation in the entire NEMS structure is reduced, which involves careful engineering of the bridge, its anchoring areas and metallization lines. Application of the so called quality factor enhanced technology, which in fact is the setup with the positive feedback loop, makes it possibly to decrease the bandwidth of the resonance frequency even further [36]. In this case however, an integration of a deflection actuator with the mechanical beam is required so that to control the structure deflection. In order to observe the resonance frequency various frequency detector can be used. The most efficient way to observe the resonance frequency change is the application of the so called phase locked loops (PLLs) systems. In the PLL systems the signal corresponding with the bridge vibration is compared with the reference signal of a digital quartz generator. The output frequency is controlled in a feedback loop so that both frequencies are equal. The resolution of the PLL detector, limited by the stability of the reference signal generator, is usually around tens of millihertz.

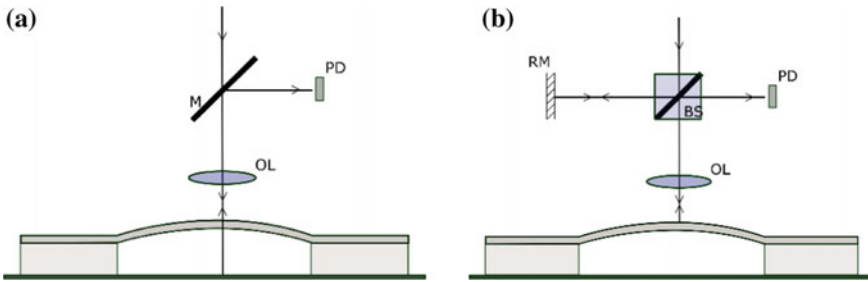


Fig. 12.4 Optical detection of NEMS deflection: **a** Michelson interferometer, **b** Fabry-Perot interferometers; *M* interferometer mirror, *OL* objective lens, *BS* beam splitter, *PD* photodetector

12.3 NEMS Detection and Actuation

12.3.1 Optical Methods

There are many approaches, making it possible to observe the NEMS displacement using optical technology. In the laboratory experiments setups basing on interferometric bulk design are often applied. In particular path stabilized Michelson interferometry and Fabry–Pérot interferometry, have been used in such measurements. In Michelson interferometers, a focused laser beam reflects from the surface of a NEMS device and interferes with a stable reference beam. In turn, in Fabry-Perot interferometers the optical cavity formed between the vibrating NEMS and its substrate modulates the optical signal on a photodetector when the nanoresonator deflects in the out-of-plane direction. In this way shot noise limited displacement sensitivities of ca. 10^{-6} nm/Hz^{0.5} Hz are routinely attainable on objects with cross sections larger than the diffraction limited optical spot in the bandwidth up to 50 MHz.

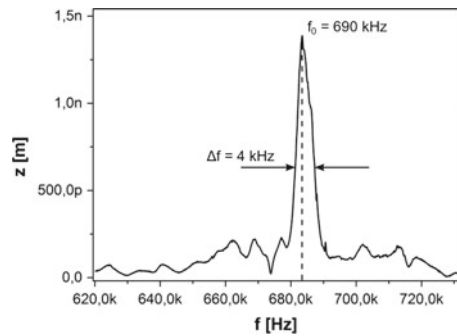
In Figs. 12.4 and 12.5 a measurement setup comprising a Michelson interferometer and the holder with a mounted silicon nitride NEMS bridge is shown. In Fig. 12.6 the resonance curve of NEMS structure is presented. A piezoelectrical actuator was used for excitation of resonance vibration of 1.5 nm amplitude. Basing on the performed experiments resonance f_0 frequency of ca. 690 kHz can be identified. The quality factor Q of the vibrations in air can be estimated of ca. 170 (Fig. 12.6).

The results obtained in this way are the quantitative ones, which is, besides the high resolution, the second advantage of the interferometrical technology. Thus, not only device diagnostics but also characterization and study of the NEMS properties can be done with high precision. The most important drawback of the described solution is related to the fact that the bulk optics, due to big mass and dimensions, cannot be integrated with the fabricated NEMS devices. From that point of view optical fibre setups are of much interest for NEMS technology. The small diameter of the optical fibre makes it possible to integrate the probing sensor i.e. optical fibre directly with a NEMS device. Such displacement sensors are often built in fibre Fabry-Perot interferometer (F-FPI) configuration in Fig. 12.7. In this setup an optical fibre is the

Fig. 12.5 Measurement setup using a bulk interferometer for silicon nitride NEMS bridge metrology

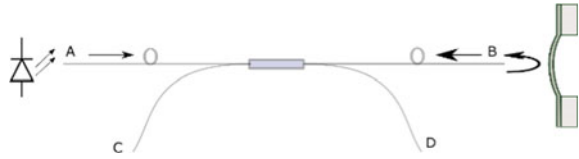


Fig. 12.6 Resonance curve of silicon nitride NEMS bridge



central part of the sensing system. A laser light source is connected to the arm *A* of the fibre coupler. The NEMS device is illuminated with the beam coming out from the arm *B* in Fig. 12.7. Part of this beam is reflected from the NEMS object and is coupled back to the fibre. Due to the difference between the refraction indexes of the air and optical fibre part of the beam emitted by the laser source is reflected from the arm *B* open end. The light beams, which are reflected from the measurement object and from the fibre open end interferes together and the interference fringes

Fig. 12.7 Fibre Fabry-Perot interferometer for NEMS deflection investigations



are observed with a photodetector connected to the arm C of the fibre coupler. As it can be seen the system is very compact and enables observation of the deflection of many NEMS devices in parallel. The proposed technology makes it possible to observe NEMS deflection with the resolution of $30 \text{ fm/Hz}^{0.5}$ [34].

If instead of a laser diode a noncoherent light source is used, the photodetector connected to the arm C detects the intensity of the beam reflected from the moving object in Fig. 12.7. In this case the photodetector signal corresponds with the distance between the optical fibre and the NEMS device. The resolution of the so called light intensity fibre optic sensor (I-FODS) is $120 \text{ pm/Hz}^{0.5}$. In comparison with the F-FPI the I-FODSs exhibits smaller resolution but can operate in the wide frequency bandwidth of up to 1 MHz. Moreover the output signal of a I-FODS is continuous which simplifies signal acquisition and data analysis, as the F-FPI requires quite cumbersome signal processing [27].

Besides optical technologies electronic systems for the detection and measurement of NEMS deflection play a very important role. Integration of a NEMS device with an electronic measurement and control environment makes it possible to develop solutions for not only laboratory but more practical applications as well [28]. Moreover, integration of the measurement and control functions in application specific integrated circuits (ASICs) enables fabrication and usage of the NEMS based devices in portable systems whose characteristics is precisely and repeatable described. The full strength of the NEMS technology can only be utilized, when it is possible not only to sense but to control the structure vibration. To control the NEMS vibration means in this case to actuate static and/or resonance structure deflection and to maintain it at the defined level with a defined speed and frequency range.

As the size of a NEMS device is being reduced and as a consequence of this operation, frequency increases the modulation of the impedance of the deflection sensing and actuation components is getting smaller. Simultaneously, the influence of stray or parasitic impedances increases which makes detection of the tiny effects very difficult. NEMS detection and actuation electronics quite often operates on its limits, which means that the electrical signals connected with the NEMS deflection are comparable with the input thermal noise of an applied amplifier and/or its bias current. Below a summary of various methods applied for the sensing and actuation of NEMS devices is presented.

12.3.2 Piezoelectric Technology

In piezoelectric materials, a mechanical stress induces electrical charge on the device electrodes. Alternatively, an applied voltage (in other words charge deposition) induces a mechanical stress in the biased crystal, which leads, depending on the elastic structure properties, to the strain of the piezoelectric system. The described technology can be used to detect and drive mechanical motion in the frequency bandwidth of up to 1 GHz. The transduction efficiency is very high and this technology is often used in MEMS devices. However, in NEMS technology the main difficulty relies in the fact that the crystal integrity must be maintained even for the structure of nanometer thickness. From that point of view, having in mind that the piezoelectric actuator must be resistant to the electrical breakdown, integration of the piezoelectric technology with NEMS devices of thickness smaller than 100 nm is quite difficult [1]. In the laboratory experiments piezoelectric actuators are very often applied to test the structure resonance properties, however in this case control of the structure vibration is difficult and cannot be done in the repeatable manner.

12.3.3 Capacitive Technology

The capacitive technology has been carried over from MEMS technology. An attractive force occurs between the plates of a capacitor when its electrodes (plates) are charged. In order to induce electrostatic force, one usually fabricates a gate electrode around the NEMS device. The most convenient and the most efficient way to excite the electrostatic force is to bias the substrate under the NEMS resonator. Many MEMS technologies can be introduced on this field, however it must be noted that stray capacitances around the NEMS device are much bigger than the capacitance between the substrate and the NEMS resonator. As the consequence the capacitive technology is less effective for higher frequencies, however solutions making it possible to control the structure deflection at frequencies of 700 MHz were reported [33]. In capacitive displacement technology, the motion of the mechanical element of a NEMS device modulates the electrical capacitance between the moving NEMS part and a fixed electrode. To detect this capacitance modulation, the NEMS capacitor is usually biased with a voltage and the current is detected using a current to voltage (I/U) converter. The biggest problem in this case is that the stray capacitances around NEMS resonator and in the I/U converter are even one order of magnitude bigger than the capacitance which is being detected. One solution to the problem is the application of a transformer ratio bridge, whose inductive arms negate the capacitive background [12, 35]. Another technology relies on implementation of the switched amplifiers using which it is possible to take into account the stray capacitances and detect very feeble signal corresponding with NEMS capacitance.

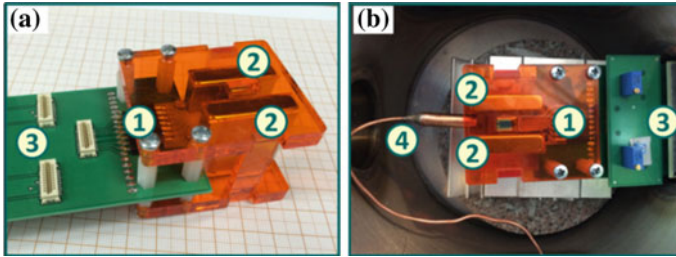


Fig. 12.8 Experimental setup of a silicon nitride bridge-electromagnetic actuation and detection. **a** Side view, **b** top view. *1* Silicon nitride bridge mounted on a printed circuit board (PCB), *2* neodymium magnets, *3* measurement and control electronic, *4* sensor for magnetic field measurements

12.3.4 Electromagnetic Technology

In the presence of a magnetic field a NEMS device deflection can be both detected and actuated by coupling of the magnetic field with a current carrying loop integrated with the NEMS device. This method is known as the electromagnetic or magnetomotive actuation and detection and can be used to drive vibration at even microwave frequencies. The drive force of a current I carrying conductor in magnetic field B is called Lorentz force F_L and can be calculated using the following formula:

$$\vec{F}_L = L_L \vec{I} \times \vec{B}. \quad (12.13)$$

where L_L is the length of the conductor. Early experiments were carried out in strong magnetic fields of few teslas generated in superconducting magnets, which made the measurement setup expensive and very large [6, 13]. Progress in fabrication of permanent magnets has made it possible to design setups of relatively small dimensions in which magnetic field of fractions of tesla are generated. In Fig. 12.8 a silicon nitride bridge with a metallization line of resistance of 120Ω placed between two neodymium magnets generating field of 0.5 T is presented. In the presented configuration Lorentz force of 140 nN can be estimated for the silicon nitride bridge of $280 \mu\text{m}$ length, drive current of 1 mA and magnetic field of 0.5 T. The estimated Lorentz force is big enough to induce NEMS structure vibration of tens of nanometers vibration amplitude. In Fig. 12.9 resonance curve of a silicon nitride film measured in vacuum of 10^{-4} Pa is presented. As it can be seen the vibration amplitude of tens of nanometers can be relatively easily measured using a Michelson interferometer. In this way static bridge deflection, which means deflection of frequency much smaller than the resonance bridge frequency, in the range of fractions of nanometers can be induced and precisely controlled.

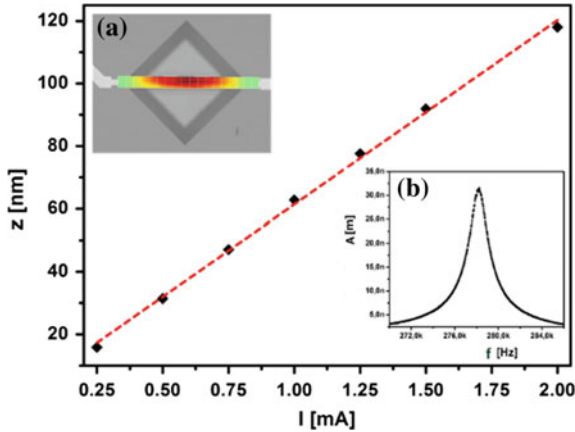


Fig. 12.9 Electromagnetically actuated resonance silicon nitride bridge vibrations

Electromagnetic technology was applied to detect the NEMS vibration for the first time in 1999 [7]. The technique is based upon the presence of a uniform static magnetic field, in which a NEMS containing a conductive wire vibrates. The time varying magnetic flux generates an induced electromotive force (EMF). For a doubly clamped bridge an EMF is given by:

$$EMF = \xi BL_L \frac{\partial x(t)}{\partial t}. \quad (12.14)$$

where ξ is a geometric factor (0.885 for a doubly clamped beam). For the beam, whose measurements were presented in Fig. 12.10 one can calculate, that the vibration period is ca. $3.5 \mu\text{s}$. If one assumes that the vibration amplitude is 40 nm at frequency of 280 kHz, the average speed of the bridge is 44 nm/ μs . For the structure length 280 μm and magnetic field 0.5 T EMF is ca. 5.5 μV . The measurement of such a low voltage is quite difficult, but having in mind that the thermal voltage noise of modern instrumental amplifiers is of few nV/Hz^{0.5} a careful engineering makes it possible to record a signal corresponding with the resonance NEMS vibration.

The electromagnetic actuation and detection of NEMS vibration can be combined, which makes the described technology extremely interesting. When a Lorentz loop is biased the structure can be excited to vibration. When it starts to oscillate in resonance a EMF voltage can be identified across the conductor. The results of the simultaneous vibration and bridge detection are presented in Fig. 12.10a, where a family of resonances was recorded for various bridge bias currents. In Fig. 12.10b the resonance curve and the relevant phase change curve are illustrated [22].

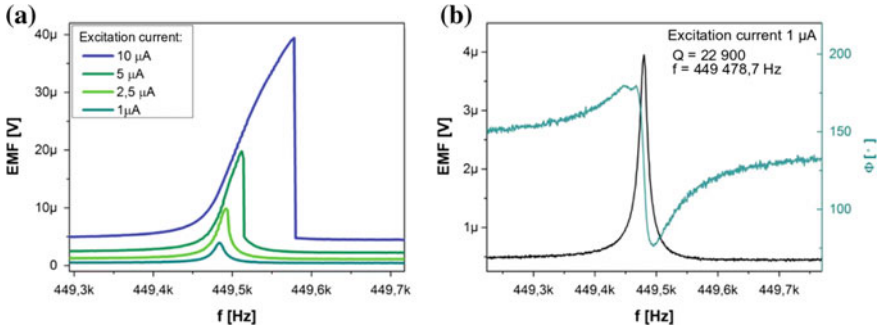


Fig. 12.10 Electromagnetic actuation and detection of electromagnetically driven and detected NEMS vibration, **a** resonance curves recorded for various drive currents, **b** resonance curve with phase shift changes

12.3.5 Piezoresistive Technology

In general piezoresistors are the sensing structures whose resistance is the function of strain. Changes of the resistance R can be described as:

$$\frac{\Delta R}{R} = \left[(1 + 2\nu) + \frac{\Delta\rho}{\rho} \right] \varepsilon = GF\varepsilon. \quad (12.15)$$

where ΔR and R are the change in resistance and total resistance respectively, ε is the applied stress, ν is the Poisson's ratio, $\Delta\rho$ and ρ is the piezoresistor resistivity respectively. The coefficient GF is the so called gauge factor, which describes the sensitivity of the strain sensing structure. When the piezoresistor is made out of metal its response is the function of the geometry changes and the term $\frac{\Delta\rho}{\rho}$ can be neglected. For metal piezoresistors GF ranges from 1.5 to 3.5 depending on material alloy. In the semiconductor piezoresistor the resistivity change $\frac{\Delta\rho}{\rho}$ becomes dominant and the geometry related term $(1 + 2\nu)$ is usually not taken into account. In this case strain induces changes in the conduction band Fermi level and as the consequence the gap size is modulated.

The piezoresistive detection scheme can be also implemented in NEMS technology. The resonator itself may be manufactured from a piezoresistive material or alternatively a piezoresistive material can be integrated with the resonator. Typically this is done at the clamping points of the resonator, where the strain is the highest. As the piezoresistive technology is the electrical one it can be easily implemented into a heterodyne down-mixing circuit where the resonant response frequency is multiplied with a bias frequency to obtain a low frequency detection signal, whose acquisition is not sensitive to parasitic capacitances. This method has been successfully applied for mass sensors and demonstrated high resolution in scanning probe microscopy (SPM) investigations [9, 31, 37]. As NEMS dimensions shrink, integration of a deflection sensing device with the nanomechanical structure is becoming challeng-

ing. Besides, solutions based on nanoelectronics FEBID techniques can be of a real support. The FEBID nanostructures are often described as composites consisting of metal nanograins embedded in non-conductive matrix whereas electron transport has been defined as inelastic tunneling process occurring among nanograins [14, 24]. This phenomenon makes it possible to apply these structures as sensors of strain, which is induced by deflection of the device integrating FEBID nanogranular piezoresistors (NGRs). The induced strain results in the modulation of the distance between embedded in an amorphous matrix metal nanograins. In this way the probability of electron tunneling among the nanograins is modulated, which in turn is observed by the changes in the resistance of the FEBID structure. As the tunneling phenomena are the quantum mechanical ones, it is expected that the deflection detection sensitivities should be very high. However, several measures must be undertaken in order to ensure stability and response repeatability of the FEBID piezoresistors. If an organometallic platinum precursor is used the fabricated FEBID piezoresistor consists of conductive platinum nanocrystallites immersed in carbon containing matrix which results in high resistivity of the deposited material and making high frequency (HF) measurements difficult. Moreover, carbon can easily oxidize in ambient conditions, which strongly influences carrier transport stability. Another important problem is that of process repeatability as the beam parameters, chemical composition and stability of the chemical precursors used for the deposition may differ from experiment to experiment [17].

The FEBID NGR structures were applied as sensors to detect the micromechanical cantilever deflection [32]. Basing on the microcantilever vibration analysis it is possible to use such structures as a mass change sensing platform. When the mass change sensitivity is concerned it is well known that the smaller platform mass corresponds with the increased mass change sensitivity. Therefore, the proper way to detect smaller mass change is to fabricate structures of smaller mass like e.g. silicon nitride bridges. However, it has to be noticed, that the smaller structures vibrate at higher frequencies and their oscillation amplitude is much smaller than that of the MEMS microcantilevers. The described features define requirements for the components detecting mechanical structure vibration, which have to exhibit high sensitivity and have to operate in wide frequency bandwidth. To the possible solutions to the presented problems belong again the FEBID technology, which ensures the high sensitivity and makes it possible to fabricate small vibration detectors.

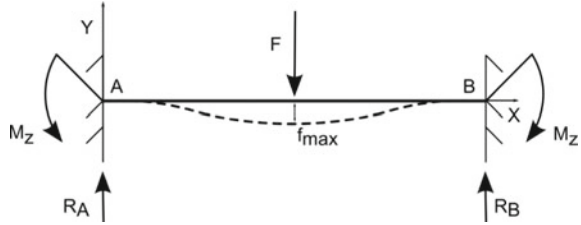
Mechanical structure of a silicon nitride bridge is shown in Fig. 12.11. Accordingly, the following formulas describe its elasticity:

$$R_A = R_B = \frac{F}{2}, \quad (12.16)$$

$$M_A = M_B = -\frac{1}{8}FL, \quad (12.17)$$

$$f_{\max} = \frac{FL^3}{192EI_z} = \frac{FL^3}{16Ewt^3}, \quad (12.18)$$

Fig. 12.11 Mechanical structure of a silicon nitride NEMS bridge



where L, w, t are the length, width and thickness of the bridge, F is the force acting in the middle of the structure, E is the Young modulus.

Stress at the bridge supporting points can be calculated using equation:

$$\sigma_{\max} = \frac{Mt}{2I_z} = \frac{3 FL}{4 wt^2}, \tag{12.19}$$

where I_z is the inertia modules of the beam: $I_z = \frac{wt^3}{12}$. Strain of the microbridge at the beam supporting points can be calculated basing on the Hooke's law:

$$\varepsilon_{\max} = \frac{1}{E}\sigma_{\max} = \frac{3 FL}{4 Ewt^2}. \tag{12.20}$$

By combining the above equations, it is possible to calculate the strain of the microbridge, when the maximal deflection is known:

$$\varepsilon_{\max} = \frac{12f_{\max}t}{L^2}. \tag{12.21}$$

Therefore, relative change of the piezoresistor resistance deposited in FEBID technology at the beam supporting points is:

$$\frac{\Delta R}{R} = GF\varepsilon_{\max} = GF\frac{3 FL}{4 Ewt^2}. \tag{12.22}$$

Application of the above equation is limited as Young's modulus of the entire bridge structure is unknown and difficult to be determined. This results from the fact that the properties of silicon nitride substrate depend on the deposition process. Moreover, the silicon nitride substrate is covered with a platinum thin film, which makes determination of the effective Young's modulus more cumbersome.

Usually, in order to obtain better sensitivity of the structure bending and to concentrate the stress in the area of the NGR piezoresistors the FIB milling will be conducted. The FIB milling is performed in close vicinity of the clamping of the microbridge in order to decrease the width of the bridge exactly in the area, where the NGR piezoresistor should be located. Shape of the FIB modified area is designed in the way to ensure the homogenous distribution of the stress along the NGR piezore-

Fig. 12.12 FIB processing of the bridges prior to the FEBID piezoresistors deposition

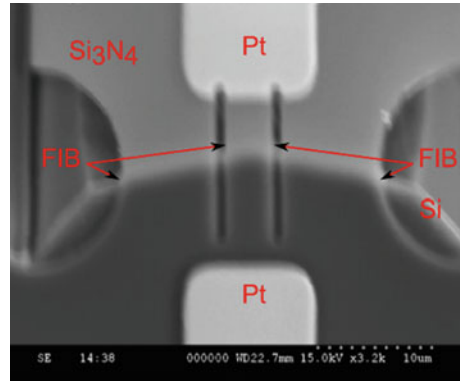
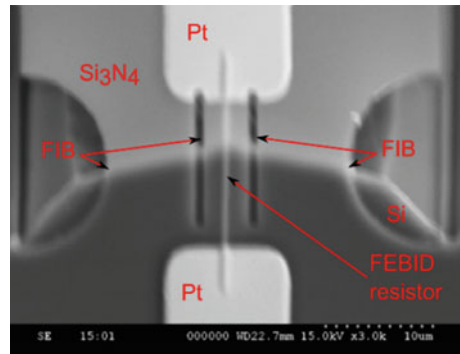


Fig. 12.13 NEMS bridge after the FIB modification with deposited FEBID resistors



sistor. As the deflection sensors receive the entire stress associated with the structure movement, their response should be the highest.

In Fig. 12.12 NEMS bridge structure with the FIB fabricated openings is shown. The FIB processed structures at the bridge supporting points and in the middle of the structure, where the FEBID piezoresistors are deposited. The FIB milling procedure was conducted in the selective way, so that to modify only the silicon nitride layer-in Fig. 12.13 the silicon substrate is clearly visible. In Fig. 12.14 the NEMS bridge after the FIB modification with the FEBID deposited piezoresistors is shown.

In order to measure the influence of the performed modifications the bridge resonance frequency were measured using a Michelson interferometer. The resonance frequency of the NEMS bridges prior to the modifications was 791 kHz. After the FIB processing the resonance frequency is decreased by around 80 kHz, which indicates decrease in the structure stiffness of ca. 20%. After the deposition of the FEBID piezoresistors the structure resonance frequencies decreases again by ca. 15 kHz. As the frequency decrease is much smaller than after the FIB processing, it can be assumed that the frequency change correlates with the structure mass loading caused by the FEBID resistors. All the resonance curves presented in Fig. 12.14 were normalized in order to present a family of resonance characteristics of the same height.

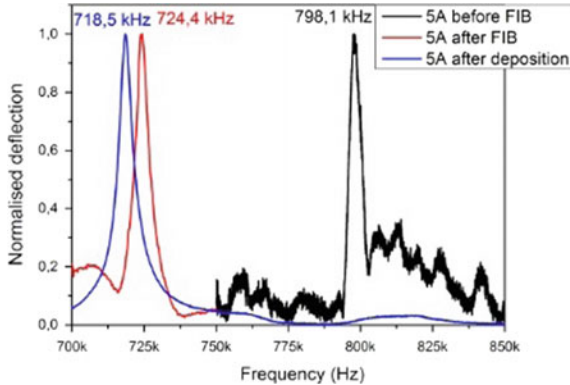


Fig. 12.14 Resonance curves of the silicon nitride bridge before and after FIB processing and after FEBID deposition of FEBID piezoresistors

The resonance properties were measured using an auxiliary piezoelectrical actuator biased with an high-resolution signal generator which excited vibration of the investigated structure.

The reference AFM silicon probes are used in the static deflection measurements of the silicon nitride bridges and the FEBID piezoresistors. In contrast to the standard AFM cantilevers, in the AdvancedTEC™ sensors the probe protrudes outside the spring beam. In this way the microprobe can be placed on the investigated bridge with high precision enabled by the optics integrated with the atomic force microscope. Moreover, in order to establish the relationship between photodiode and piezoelectric actuator displacement signals the cantilever deflection detector sensitivity was determined, when the cantilever was pushed against hard surface as it was described in [36]. In this way the so called load force (LF) curves can be recorded in the contact mode (CM) atomic force microscopy (AFM) technology and used for the precise and quantitative structure characterization. The AFM machine was integrated with the measurement equipment (current to voltage (I/U) converter Keithley 428, multimeter Agilent 2001) making it possible to record the changes of the FEBID piezoresistors resistance change under the load of the reference cantilever.

In Fig. 12.15 the measurement architecture is presented. The FEBID piezoresistors are biased using an integrated voltage source, the voltage response of the I/V converter is measured by the multimeter and recorded by the host PC computer. The proposed measurement architecture offers the highest possible resolution of the resistance change detection. In Fig. 12.16 the result of the performed investigation is shown. The microbridge was loaded with the reference cantilever [36]. The microstructure was deflected by 1 μm in every step. The resistance changes were approximated in order to calculate GF , which is the measure of the sensitivity of the deflection detection.

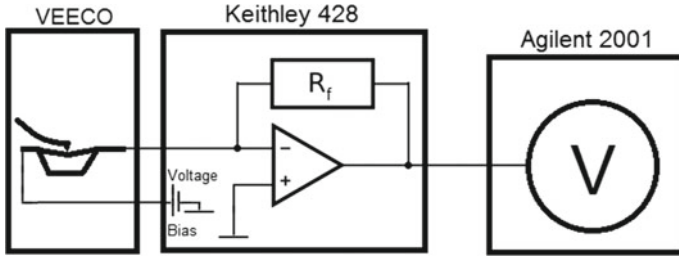
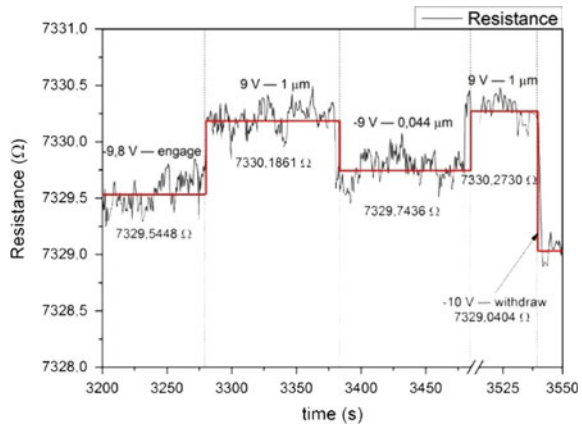


Fig. 12.15 Measurement setup for the characterization of the FEBID piezoresistors

Fig. 12.16 Measurement of the FEBID resistance under microstructure loading/test deflection



The elongation of the bridge can be estimated according to the scheme:

- (a) longitudinal elongation of the bridge under the load force:

$$L_{end} = 2 \times \sqrt{\left(\frac{1}{2}L_0\right)^2 + d^2}, \tag{12.23}$$

L_{end} —is the length of the microbridge after structure loading, L_0 —the length before loading, d —the test loading

- (b) gauge factor GF :

$$GF = \frac{\frac{\Delta R}{R}}{\frac{\Delta L}{L_0}}, \tag{12.24}$$

$$\Delta L = L_{end} - L_0, \tag{12.25}$$

$$\Delta R = R_{end} - R_0, \tag{12.26}$$

where R_{end} —is the resistance after loading, R_0 —is the resistance before loading.

Basing on the above described calculations the GF of the platinum/carbon FEBID piezoresistors varies in the range from 4 to 6. The obtained result indicates that the measurement sensitivity is bigger than in the case of the bulk metal piezoresistors, when the GF varies in the range from 2 to 4. In addition, the performed experiments clearly show, that the proposed technology makes it possibly to fabricate and deposit strain sensors on the NEMS devices, at the positions where the highest stress occurs. The resolution, with which such a deposition can be done is of tens of nanometers indicating, that the described process is very attractive for the nanotechnological applications. Usage of the AFM based techniques makes it possible to determine the basic parameter of the developed devices.

12.4 Summary

NEMS technology opens new fields in nanotechnology. The extremely small dimensions of the fabricated devices make it possible to define the place of the investigations and measurement with the highest possible resolution. In this way investigations of the quantum phenomena will be enabled in many research laboratories active on this area. The growing range of NEMS applications is correlated with the need for device characterization and measurements. This symmetrical relation stimulates the progress in the nanotechnology and micro- and nanofabrication.

Acknowledgements This work was supported by the Wrocław University of Science and Technology (WUST) statutory grant. The author would like to thank all the coworkers of the Nanometrology Division of the Faculty of Microsystems Electronics and Photonics at the WUST for their support and collaboration.

References

1. Bannon F, Clark J, Nguyen C (2000) High-Q HF microelectromechanical filters. *IEEE J Solid-State Circuits* 35(4):512–526
2. Barton RA, Ilic B, Van Der Zande AM, Whitney WS, McEuen PL, Parpia JM, Craighead HG (2011) High, size-dependent quality factor in an array of graphene mechanical resonators. *Nano Lett* 11(3):1232–1236
3. Belic D, Shawrav M, Gavagnin M, Stöger-Pollach M, Wanzenboeck D, Bertagnolli E (2015) Direct-write deposition and focused-electron-beam-induced purification of gold nanostructures. *ACS Appl Mater Interfaces* 7(4):2467–2479
4. Chen C, Hone J (2013) Graphene nanoelectromechanical systems. *Proc IEEE* 101(7):1766–1779
5. Chen C, Rosenblatt S, Bolotin KI, Kalb W, Kim P, Kymissis I, Hone J (2009) Performance of monolayer graphene nanomechanical resonators with electrical readout. *Nat Nanotechnol* 4(12):861–867
6. Cleland A, Roukes M (1996) Fabrication of high frequency nanometer scale mechanical resonators from bulk Si crystals. *Appl Phys Lett* 69:2653
7. Cleland A, Roukes M (1999) External control of dissipation in a nanometer-scale radiofrequency mechanical resonator. *Sens Actuators A* 72(3):256–261

8. Goniszewski S, Gallop J, Adabi M, Gajewski K, Shaforost O, Klein N, Hao L (2015) Self-supporting graphene films and their applications. *IET Circuits Devices Syst Spec* 9:420–427
9. Gotszalk T, Grabiec P, Rangelow I (2003) Calibration and examination of piezoresistive Wheatstone bridge cantilevers for scanning probe microscopy. *Ultramicroscopy* 97(1–4):385–389
10. Grabiec P, Gotszalk T, Radojewski J, Edinger K, Abedinov N, Rangelow IW (2002) SNOM/AFM microprobe integrated with piezoresistive cantilever beam for multifunctional surface analysis. *Microelectron Eng* 61–62:981–986
11. Hoefflich K, Jurczyk J, Zhang Y, Puydinger M, Goetz M, Guerra-Nunez C, Best J, Kapusta Cz, Utke I (2017) Direct electron beam writing of silver-based nanostructures. *ACS Appl Mater Interfaces* 9:24071–24077
12. Huang S, Stott A, Green R, Beck M (1988) Electronic transducer for measurement of low value capacitances. *J Phys E: Sci Instrum* 21:242
13. Huang X, Zorman C, Mehregany M, Roukes M (2003) Nanoelectromechanical systems: nanodevice motion at microwave frequencies. *Nature* 421:6922
14. Huth M (2010) Granular metals: from electronic correlations to strain-sensing applications. *J Appl Phys* 107:113709
15. Ko WH (2007) Trends and frontiers of MEMS. *Sens Actuators A* 136(1):62–67
16. Koops H, Fukuda H (2016) Giant current density via indirect exciton orbit overlapping in polarized nano-granular materials. *J Vac Sci Technol* 33(2):02B108
17. Lewis B, Mound B, Srijanto B, Fowlkes J, Pharr G, Rack P (2017) Growth and nanomechanical characterization of nanoscale 3D architectures grown via focused electron beam induced deposition. *Nanoscale* 9:16349–16356
18. Li M, Tang HX, Roukes ML (2007) Ultra-sensitive NEMS-based cantilevers for sensing, scanned probe and very high-frequency applications. *Nat Nanotechnol* 2(2):114–120
19. Llobet J, Gerboles M, Sansa M, Bausells J, Borrise X, Perez-Murano F (2015) Fabrication of functional electromechanical nanowire resonators by focused ion beam implantation. *J Micro-Nanolithography MEMS and MOEMS* 14(3)
20. Llobet J, Sansa M, Gerbolés M, Mestres N, Arbiol J, Borrise X, Pérez-Murano F (2014) Enabling electromechanical transduction in silicon nanowire mechanical resonators fabricated by focused ion beam implantation. *Nanotechnology* 25:135302
21. López-Polín G, Gómez-Navarro C, Parente V, Katsnelson MI, Pérez-Murano F, Gómez-Herrero J (2015) Increasing the elastic modulus of graphene by controlled defect creation. *Nat Phys* 11:26
22. Moczala M, Babij M, Kwoka K, Piasecki T, Sierakowski A, Gotszalk T (2019) Resolution improvement in electromagnetically actuated Wheatstone bridge configuration micromechanical resonators. *Sens Actuators A* 284:181–185
23. Moczala M, Kopiec D, Sierakowski A, Dobrowolski R, Grabiec P, Gotszalk T (2014) Investigations of mechanical properties of microfabricated resonators using atomic force microscopy related techniques. *Microelectron Eng* 119:164–168
24. Moczala M, Kwoka K, Piasecki T, Kunicki P, Sierakowski A, Gotszalk T (2017) Fabrication and characterization of micromechanical bridges with strain sensors deposited using focused electron beam induced technology. *Microelectron Eng* 176:111–115
25. Moczala M, Sierakowski A, Dobrowolski R, Grabiec P, Gotszalk T (2013) Fabrication and measurement of micromechanical bridge structures for mass change detection. *Proceedings SPIE*, vol 8902, p 89021.s
26. Nieradka K, Kopiec D, Małozieć G, Kowalska Z, Grabiec P, Janus P, Gotszalk T (2012) Fabrication and characterization of electromagnetically actuated microcantilevers for biochemical sensing, parallel AFM and nanomanipulation. *Microelectron Eng* 98:676–679
27. Orłowska K, Słupski P, Świątkowski M, Kunicki P, Sankowska A, Gotszalk T (2015) Light intensity fibre optic sensor for MEMS displacement and vibration metrology. *Opt Laser Technol* 65:159–163
28. Orłowska K, Świątkowski M, Kunicki P, Kopiec D, Gotszalk T (2016) High-resolution and wide-bandwidth light intensity fiber optic displacement sensor for MEMS metrology. *Appl Opt* 55(22):5960–5966

29. Polski Komitet Normalizacyjny (2010) Międzynarodowy słownik metrologii. Pojęcia podstawowe i ogólne oraz terminy z nimi związane (VIM). PKN-ISO/IEC Guide 99
30. Puydinger M, Velo M, Domingos R, Zhang Y, Maeder X, Guerra-nun C, Be F (2016) Annealing-based electrical tuning of cobalt–carbon deposits grown by focused-electron-beam-induced deposition. *ACS Appl Mater Interfaces* 8:32496–32503
31. Rangelow IW, Grabiec P, Gotszalk T, Edinger K (2002) Piezoresistive SXM sensors. *Surf Interface Anal* 33:59–64
32. Schwalb Ch, Grimm Ch, Baranowski M, Sachser R, Porrati F, Reith H, Das P, Müller J, Völklein F, Kaya A, Huth M (2010) A tunable strain sensor using nanogranular metals. *Sensors* 10:9847–9856
33. Sekaric L, Parpia JM, Craighead H, Feygelson T, Houston B, Butler J (2002) Nanomechanical resonant structures in nanocrystalline diamond. *Appl Phys Lett* 81:4455–4457
34. Smith D, Pratt J, Howard L (2009) A fiber-optic sinterferometer with subpicometer resolution for dc and low-frequency displacement measurement. *Rev Sci Instrum* 80(3):035105
35. Swiatkowski M, Wojtuś A, Wielgoszewski G, Rudek M, Piasecki T, Jozwiak G, Gotszalk T (2019) A low-noise measurement system for scanning thermal microscopy resistive nanoprobe based on a transformer ratio-arm bridge. *Meas Sci Technol* 29:045901
36. Tamayo J (2005) Study of the noise of micromechanical oscillators under quality factor enhancement via driving force control. *J Appl Phys* 97(4):1–10
37. Tortonese M, Barrett R, Quate C (1993) Atomic resolution with an atomic force microscope using piezoresistive detection. *Appl Phys Lett* 62(8):834–836
38. Zaborowski M, Dumania P, Tomaszewski D, Czupryniak J, Ossowski T (2012) Development of Si nanowire chemical sensors. *Proc Eng* 47(1000):1053–1056. <https://doi.org/10.1016/j.proeng.2012.09.331>